Surface & Coatings Technology 205 (2010) 158–167

Contents lists available at ScienceDirect

Surface & Coatings Technology

journal homepage: www.elsevier.com/locate/surfcoat

Effects of thickness and cycle parameters on fretting wear behavior of CVD diamond coatings on steel substrates

Qiuping Wei [a,b,c], Z.M. Yu [a,*], Michael N.R. Ashfold [b], Z. Chen [a], L. Wang [a], L. Ma [c]

[a] School of Materials Science and Engineering, Central South University, Changsha, 410083, PR China
[b] School of Chemistry, University of Bristol, Bristol BS8 1TS, United Kingdom
[c] State Key Laboratory of Powder Metallurgy, Central South University, Changsha, 410083, PR China

ARTICLE INFO

Article history:
Received 23 March 2010
Accepted in revised form 10 June 2010
Available online 18 June 2010

Keywords:
CVD diamond films
Steel substrates
Interlayer
Fretting wear

ABSTRACT

Diamond films have been grown on carbon steel substrates by hot filament chemical vapour deposition (CVD) methods. A Co-containing tungsten-carbide coating prepared by high velocity oxy-fuel spraying was used as an intermediate layer on the steel substrates to minimize the early formation of graphite (and thus growth of low quality diamond films) and to enhance the diamond film adhesion. The effects of thickness and cycle parameters on adhesion, tribological behaviour and electrochemical treatment of the diamond film were investigated. The diamond films exhibit excellent adhesion under Rockwell indentation testing (1500 N load) and in high-speed, high-load, long-time reciprocating dry sliding ball-on-flat wear tests against a Si_3N_4 counterface in ambient air (500 rpm, 200 N, 300000 cycles). Time modulated CVD (wherein the CH_4 fraction in the process gas mixture is cycled in time) is shown to yield diamond films offering an exceptional combination of low friction, high hardness, high wear resistance, as well as promising corrosion resistance.

1. Introduction

Wastage due to the combined effects of wear and corrosion has received much attention in recent years, due to the prevalence of such problems in many diverse environments. As engineering applications become ever more demanding, there is an increasing requirement for composite coatings that both protect the substrate to retain its mechanical strength, but also enhance the resistance of the substrate to wear and corrosion [1]. Alloy steels are among the most commonly used and cost-effective structural materials in modern industry. However, when steel is used for critical wear resistant components and machining tools in harsh (wear, corrosive and erosive) environments, accelerated damage usually occurs. Diamond has exceptional mechanical and corrosion resistant properties [2,3], i.e. the highest hardness and wear resistance, the lowest friction coefficient, as well as chemical inertness to aqueous corrosion, which make diamond films grown by chemical vapor deposition (CVD) potentially ideal coatings for wear resistant components and machining applications [4], including bearings, mechanical seals, cutting tools, and gears. Well-adhered diamond films deposited on steel surfaces can lead to major improvements in the life and performance of steel tools, since the early failure of such tools is usually initiated at the outermost surface. Despite the great industrial potential, practical applications of this technique have been limited due to difficulties in achieving satisfactory diamond film adhesion to the steels, as a result of several limiting factors [5–8]. These include: (1) iron catalyses graphite formation at diamond/steel interfaces during the CVD process; (2) the high solubility of carbon in the iron fcc phase leads to prolonged diamond nucleation times; (3) the large difference in the coefficients of thermal expansion between diamond and steel may induce high stress within the deposited diamond films. As direct diamond coating of steel is very difficult, modification of the surface, or the use of interlayers, in order to improve the quality and adhesion of any diamond coating is indispensable. The use of intermediate layers traditionally involves complex and costly multi-step procedures, and the adhesion at both the substrate/interlayer and the interlayer/diamond interfaces has to be simultaneously guaranteed. Different kinds of steel substrate modifications and the application of various interlayers have been reported [9]. Buijnsters *et al.* [10] obtained low-residual-stress films on ferritic tool and AISI type 316 austenitic stainless steels by a boriding pretreatment. Chromium nitride or carbide coatings have been used extensively as interlayers for diamond deposition on steel substrates, and can lead to improved film quality and adhesion [11–21]. Haubner *et al.* [21] investigated diamond deposition on steel substrates first coated with industrially available intermediate PVD-layers (CrN, TiAlN, TiCN, TiN, WC/C), with particular reference to nucleation and growth and, additionally, the influence of the intermediate layers on carbon diffusion. Nucleation rates were found to be low, and no diamond coatings were observed. For industrial applications, enhancing nucleation remains an issue, as does the adhesion of any diamond layer to the various intermediate layers.

The wear mechanisms and the electrochemical behaviour of thin diamond films have both been the subject of many previous investigations

* Corresponding author. Tel.: +86 731 8830335; fax: +86 731 8876692.
E-mail address: zhiming@mail.csu.edu.cn (Z.M. Yu).

0257-8972/$ – see front matter © 2010 Elsevier B.V. All rights reserved.
doi:10.1016/j.surfcoat.2010.06.026

[22–37]. Natural diamond is a chemically-inert and wear resistant material in a wide range of aggressive environments, but we are aware of no publications investigating how the erosion or corrosion of continuous polycrystalline diamond films affects their adhesion to steel substrates. Such studies are important, given that many of the more obvious tribological applications of such coatings involve corrosive and erosive environments. In the present work, a Co-containing tungsten carbide (WC-Co) coating has been thermally sprayed on carbon steel using a high velocity oxy-fuel (HVOF) spray technique to act as an intermediate layer prior to diamond film deposition, in order to improve the quality and adhesion of the latter. Gowri *et al.* [38] have found that dense and adherent diamond coatings can be deposited by a two-step hot filament (HF) CVD method on high speed steel that was previously borided or coated with a WC-Co interlayer. The present study investigates how the thickness of CVD diamond coatings on steel substrates affects their fretting wear, describes some preliminary study of their electrochemical corrosion and how this can affect the diamond film adhesion, and ends by identifying a coating route that simultaneously guarantees high adhesion, low friction, high wear resistance, and suggest promising corrosion resistance.

2. Experimental details

Diamond films were deposited in a HF assisted CVD reactor designed and constructed in the Department of Physics at the Royal Institute of Technology, Stockholm (Sweden), [39], and subsequently transferred to Central South University.

The films were grown on carbon steel plates, and a Co-containing tungsten carbide (WC-Co) coating was used as an interlayer to improve the nucleation, quality and adhesion of the diamond film. The flat specimens used in this study were $50\times30\times5$ mm^3 AISI 1085 carbon steel plates coated with a WC-Co interlayer (~400 μm in thickness) by HVOF. The WC-Co blends used here typically comprised 85-90% WC and 10-15% Co powder (powder size ~2-5 μm), and the spraying parameters were: oxygen flow 57 m^3/h; spray distance 30 cm; fuel rate 23 liters per hour. The substrates were then cut into smaller plates of dimension $10\times10\times5$ mm^3 by spark cutting. Due to the high roughness of the sprayed WC-Co interlayer, the specimens were polished with diamond polishing agent; the final interlayer thickness after polishing was ~200 μm and the surface roughness ~3 μm. All specimens were then etched using the following two-step pretreatment: (i) etching by Murakami's reagent (10 g $K_3[Fe(CN)_6]$ + 10 g KOH + 100 ml H_2O) for 3 minutes in an ultrasonic vessel [40]; (ii) removal of the surface Co by etching in an acidic solution of hydrogen peroxide (2 ml 96 wt.% H_2SO_4 + 2 ml 68 wt.% HNO_3 + 20 ml 40% w/v H_2O_2 + 40 ml H_2O) for 2 minutes. Prior to diamond deposition, all pretreated specimens were first abraded ultrasonically in a suspension of diamond powder (<500 nm particle size) in acetone for 30 minutes. This treatment, often described as 'seeding', encourages the subsequent inhomogeneous nucleation of diamond during CVD — either by implanting ultrafine diamond fragments into the substrate surface, or by creating suitable surface defects. Table 1 shows parameters which were typically maintained constant for each specimen and deposition. At least three specimens of each type were deposited under the same conditions. The results presented in this article are representative of those found for all specimens subjected to a given parameter set.

Table 1
Experimental parameters used for diamond film deposition on carbon steel substrates with a WC-Co interlayer.

Specimen No.	D_1	D_2	D_3	D_4	D_5	D_6
Substrate pretreatment					two-step pretreatment	
Filament-substrate distance (mm)					8 ± 2	
Substrate temperature (°C)					750 ± 50	
CH_4/H_2 ratio (vol. %)	3				3 (20 min)/1 (20 min)	3 (10 min)/1 (30 min)
Deposition pressure (kPa)					3	
Total gas flow rate (sccm)					50	
Deposition time (min)	180	300	480	2760	320	600

The surface and cross-section morphologies of the diamond films were characterized by scanning electron microscopy (SEM, FEI, Sirion200 Field-emission SEM and Quanta200 Environmental SEM), and their quality assessed by Raman spectroscopy (LabRAM HR800), at an excitation wavelength of 488 nm (argon ion laser, output power of 100 mW). Electrochemical investigations of the diamond coated steel specimens were conducted in a glass cell with a platinum counter electrode and a saturated calomel electrode (SCE) as reference using a galvanostat/potentiostat. The specimens were tested in 3.5 mol/L aqueous NaCl solutions at room temperature. Open circuit potential curves were measured after immersing the coated layers in the solution for 30 min to ensure potential stabilization. The potentiodynamic polarisation curves were recorded at a scan rate of 1.0 mV/s, in both the forward and reverse directions, starting from cathodic potentials. For all specimens, only the diamond coated top surfaces were exposed to the solution; the other faces (including the backsides) were protected by a corrosion resistant lacquer. The current densities were thus obtained by dividing the measured currents by the surface areas actually exposed to the solution.

The adhesion and tribological properties of the diamond-coated steel substrates were characterized using a Rockwell hardness tester with a Brale diamond indenter (angle = 120°, radius = 0.2 mm) at loads of 600 N, 1000 N and 1500 N, respectively, and by reciprocating fretting tests. Friction and wear tests were conducted using a ball-on-disk tribometer (High Load, Heavy Duty Tribometer, UMT-3, CETR, USA) with pairs of silicon nitride (Si_3N_4) balls and diamond-coated substrates. The measurements were made in open air, at ambient temperature and at a relative humidity (RH) of (65 ± 5) %. A Si_3N_4 ball (9.5 mm in diameter) with a surface finish of better than 0.1 μm was loaded on the diamond coated flat steel specimen as counterface materials mounted on a horizontal translation table. Loads (F) of, respectively, 5, 20, 50 and 200 N were applied to the Si_3N_4 ball while the test specimens were subjected to a reciprocating displacement with the sliding velocity (V) set at either 500 or 1000 rpm. The sliding distance of the Si_3N_4 ball vs. diamond-coated steel substrates in the reciprocating fretting tests was

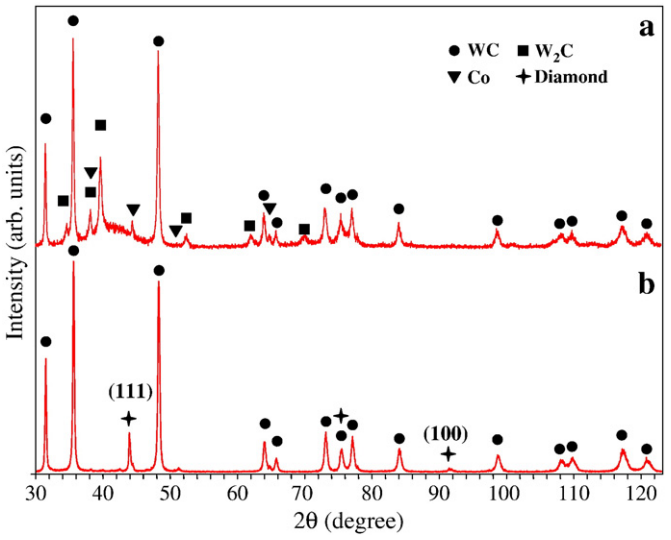

Fig. 1. X-ray diffraction patterns of (a) the as-coated WC-Co interlayer on a carbon steel substrate, (b) a D_1 specimen.

~4 mm. The coefficient of friction (COF) was obtained from the measurement of the tangential force exerted on the ball during sliding. The COF signal was integrated with a time constant of 0.01 s.

3. Results and Discussion

During thermal spraying, the cobalt phase in a WC-Co particle starts to melt as it is heated in the hot gas jet and the WC grains begin to dissolve within it. The periphery of the semi-molten particle becomes decarburized by oxidation, promoting further WC dissolution. The molten or semi-molten particles then impact on the substrate to form a laminar coating composed of many layers, called 'splats'. Particle quenching upon impact with the substrate results in precipitation of W_2C and, possibly, W from the melt, depending on the local melt composition [41]. In the present work, the HVOF WC-Co coating mainly consists of the following phases: WC, a small amount of Co, and a trace amount of W_2C demonstrated by the XRD data shown in Fig. 1(a). No elemental W phase could be detected from this analysis. Thermal spray coatings normally also contain non-uniform distributions of carbide and cobalt 'lakes' [42]. Various researchers have compared sintered WC-Co with thermally sprayed WC-Co with a view to understanding the microstructure-performance relationships and thereby improving the performance of coated systems to match that of sintered surfaces [1]. The tribological behavior, and the abrasion and erosion resistance, of these thermally sprayed WC-Co coatings is generally poorer than that of bulk sintered WC-Co — reflecting the inhomogeneous microstructure and the phase transformations of the starting material, which lead to wide variations in mechanical properties and corrosion resistance [1,43]. Wayne *et al.* [43] deduced that, for coatings, a porous structure causes poor intersplat bonds and weaker carbide to matrix bonding which, in turn, reduces the fracture toughness, and hence the erosion resistance. Thakare *et al.* identified preferential corrosion along the periphery of the carbide grain [42], *i.e.* in regions which are likely to have formed W_2C, and corrosion of the decarburized surface of the grain (which gradually progresses towards the carbide grain centre). Lima *et al.* find that an

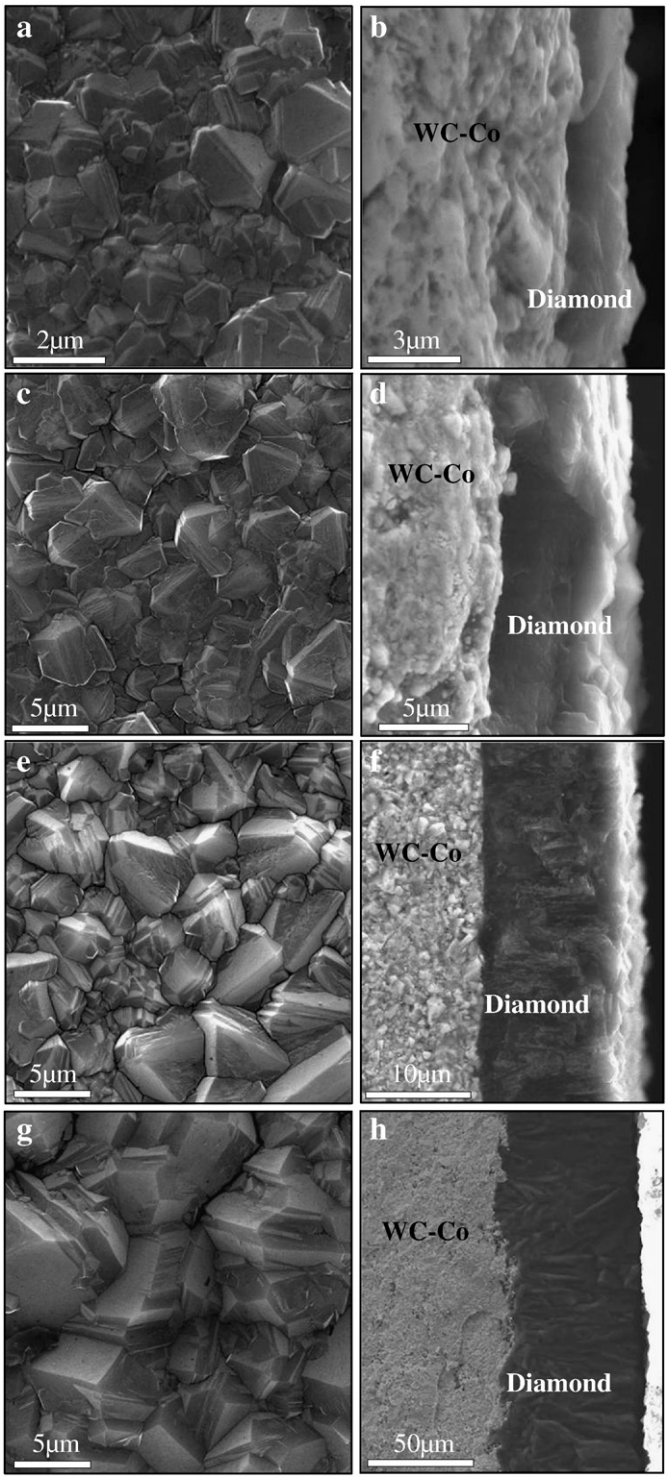

Fig. 2. Representative SEM images of diamond films deposited on specimens (a, b) D_1, (c, d) D_2, (e, f) D_3 and (g, h) D_4. Left images are top views, while right images are cross-sections.

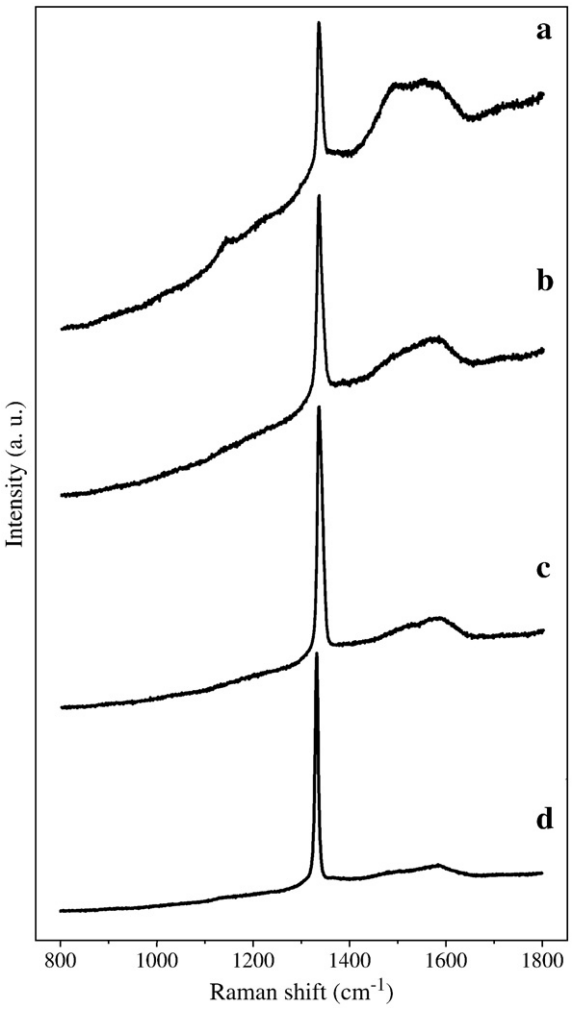

Fig. 3. Raman spectra of diamond films deposited on (a) D_1, (b) D_2, (c) D_3 and (d) D_4 specimens.

increasing W_2C fraction is probably the most significant factor in reducing the fracture toughness of WC-Co coatings, and that appropriate post-heat treatments can improve the indentation toughness of thermally sprayed WC-Co coatings [44]. Typical substrate temperatures for diamond deposition are in the range $600 \leq T_s \leq 950$ °C. Processing such thermally sprayed WC-Co coatings in a CH_4/H_2 atmosphere under diamond CVD conditions (*i.e.* high T_s) is very much like a uniform heat treatment. Diffusion of active atomic carbon encourages transformation of $W_2C \rightarrow WC$ [45], while Co diffusion tends to homogenize the microstructure and phase composition, with the result that the WC-Co interlayer develops a similar microstructure and phase composition to that of bulk sintered WC-Co [4] (see Fig. 1(b)), and the mechanical properties and corrosion resistance of the interlayer will be enhanced.

Fig. 2 shows representative surface and cross-section SEM images of diamond films with different thicknesses. The SEM images show dense and homogeneous diamond coatings and typical diamond crystallite morphologies. With increasing growth time, the diamond film thickness and the average diamond crystallite grain size increases. No ball-shape cobalt particles, such as reported elsewhere [46], were evident on the surface of any of the diamond films grown in this work.

Raman spectra of films deposited on specimens D_1, D_2, D_3 and D_4 are shown in Fig. 3. The diamond peaks in these spectra are somewhat blue-shifted with respect to the peak position in a natural, stress-free diamond sample (1332.2 cm^{-1}), which is the result of residual, compressive stress attributable to the mismatch in thermal expansion between the substrate and the diamond film. The ratio of the intensities of the sp^2 characteristic feature at ~1550 cm^{-1} and the diamond peak at ~1340 cm^{-1} decreases with increasing growth time, indicating a reduction of the relative amount of sp^2-bonded carbon and an improvement in quality with increasing diamond film thickness. Such a finding accords with the SEM images (Fig. 2), which showed the grain size increasing with deposition time. sp^2-bonded carbons are found predominantly at the grain boundaries, [24] the relative density of which (in any given laser probe area) will be greatest in the case of small grain (*i.e.* short growth time) material.

Rockwell indentation tests were performed with loads of, respectively, 600 N, 1000 N and 1500 N. Results obtained with the 1500 N load are shown in Fig. 4. No flaking-off of the diamond film was observed around the indentation on any of the specimens, demonstrating the good adhesion of all of the diamond films.

Fig. 5 shows the electrochemical behaviour of the base carbon steel substrate, the steel substrate coated with the WC-Co interlayer, and diamond films (of different thickness) on steel substrates coated with the WC-Co interlayer, upon potentiodynamic polarisation in an aerated 3.5 mol/L NaCl solution. The potential corresponding to the minimum current density is known as the equilibrium corrosion potential (E_{corr}). Compared to the bare carbon steel reference specimen, E_{corr} is shifted in the positive direction for both the WC-Co interlayer coated carbon steel substrate and the diamond coated substrate; the magnitude of this shift for the diamond coated carbon steel substrate with a WC-Co interlayer is much greater however, and the magnitude of this shift increases as the thickness of the diamond film increases. No evidence of attack or morphological changes of the diamond films were observable after anodic polarisation for 30 min.

As described before, during thermal spraying, as a WC-Co particle is heated in the hot gas jet, the cobalt phase melts and the WC grains begin to dissolve within it. Molten or semi-molten particles impact on the substrate to form a laminar coating composed of many layers, called 'splats'. Some of the incident particles overlap previous splats, some connect to previous splats, and others land within the intervening spaces. As Fig. 6(a) illustrates, an incident splat can bridge between existing splats to form gaps of differing sizes (*e.g.* style A and B) – as reported many times previously [1,42]. Thakare *et al.* also found an inhomogeneous distribution of carbide-rich and binder-rich areas within the coating, and that the carbide size distribution within the coating was non-uniform, with larger carbide components concentrated towards the centre of the splats and finer carbides along the splat boundary [42]. Direct deposition of an adherent diamond coating on Co-containing cemented carbide is challenging because of the presence of cobalt at the substrate surface. This limits diamond nucleation, since Co can catalyze the formation of graphite and other non-diamond carbon phases, leading to very low film adhesion [46,47]. With appropriate chemical pretreatment, however, diamond nucleation on, and adhesion to, a WC-Co interlayer can be greatly improved. The previously described two-step pre-treatment

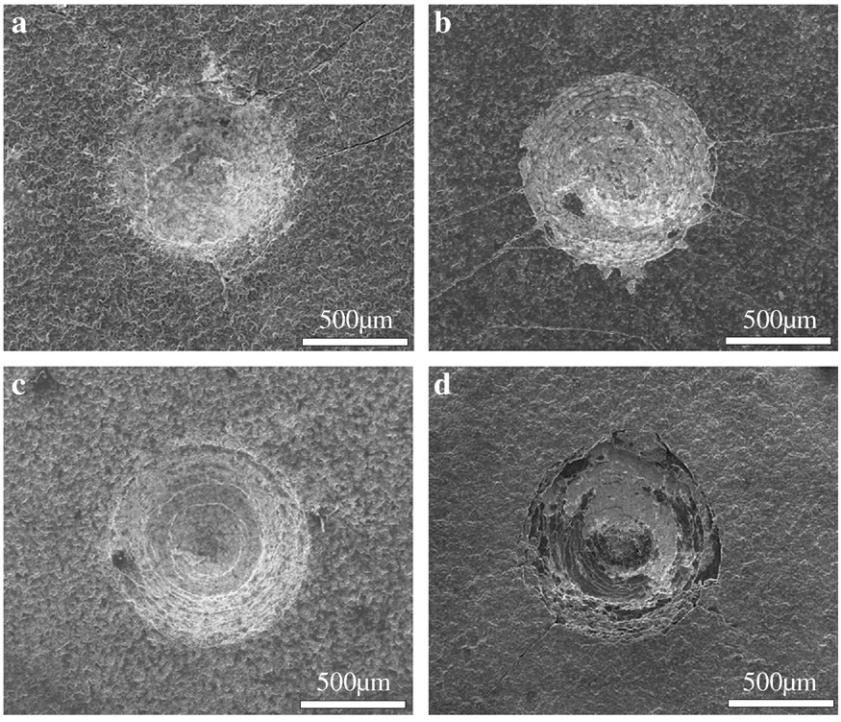

Fig. 4. SEM images of Rockwell indentations of (a) D_1, (b) D_2, (c) D_3 and (d) D_4 specimens under a load of 1500 N.

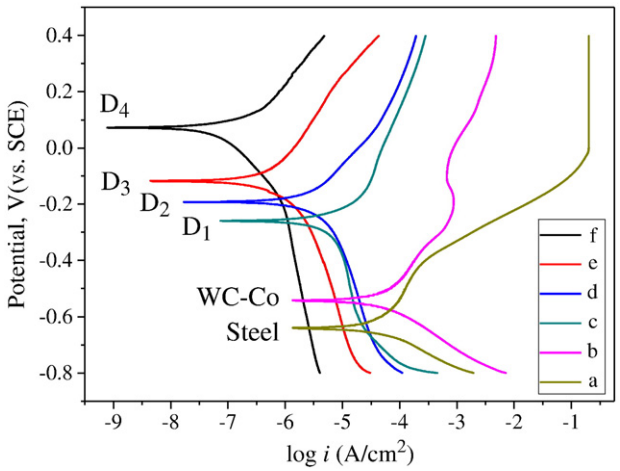

Fig. 5. Comparison of potentiodynamic polarization curves of: (a) the carbon steel substrate; (b) the WC-Co interlayer coated carbon steel substrate; and diamond films deposited on specimens (c) D_1, (d) D_2, (e) D_3 and (f) D_4 in the aerated 3.5 mol/L NaCl solution.

yields a Co-deficient, porous, corrosion layer on the substrate surface (illustrated schematically in Fig. 6(b)). Given the porosity and the inhomogeneous distribution of binder-cobalt areas within the initial WC-Co coating formed by HVOF, it is essentially impossible not to end up with a rough surface after chemical pre-treatment (as shown in Fig. 6(c)). Most Co agglomerates will transform into surface pits during the two-step etching. Surface defects created by the two-step chemical pre-treatment enhance diamond nucleation, but also result in a non-uniform distribution of nucleation sites – thereby increasing the surface roughness further [4].

A diamond film grown on such a rough surface will initially tend to replicate the surface topology (as shown schematically in Fig. 7(a)), [4] but the memory of the underlying morphology will fade as the growth time is extended. The surface topology of thicker diamond films will progressively be determined by the CVD conditions, rather than the roughness of the underlying substrate – as illustrated in Fig. 8(a). Rougher surfaces tend to induce increased ploughing (and hence display higher friction) under reciprocating fretting wear testing. A well-adhered thin diamond film will be progressively worn down during reciprocating slide testing (as illustrated schematically in Fig. 7(b) and in practice by the SEM images shown in Fig. 7(c) and (d)); fragments may also break off if the horizontal shearing force exceeds the fracture strength of the WC-Co coating or the bonding strength of the diamond film to the underlying WC-Co coating. The SEM image shown in Fig. 7(e) shows a region of the WC-Co interlayer exposed by such a fracture. The horizontal shearing force associated with reciprocating slide testing is generally distributed more widely in the case of well-adhered thicker diamond film. Wear in this case is seen to involve initial removal of surface asperities (by fracture or

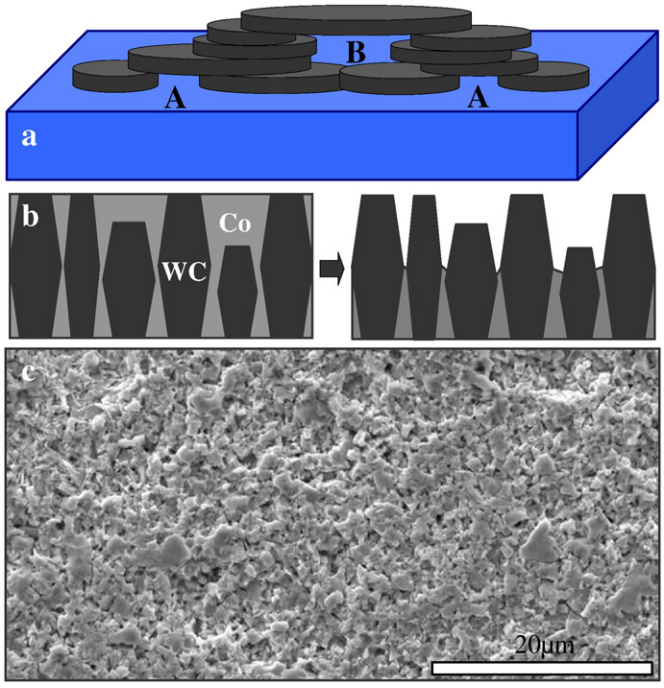

Fig. 6. Models of defects and pores formed by (a) thermal spray deposition and (b) before and after chemical etch pre-treatment. (c) shows an SEM image of a typical HVOF WC-Co surface after two-step chemical pretreatment.

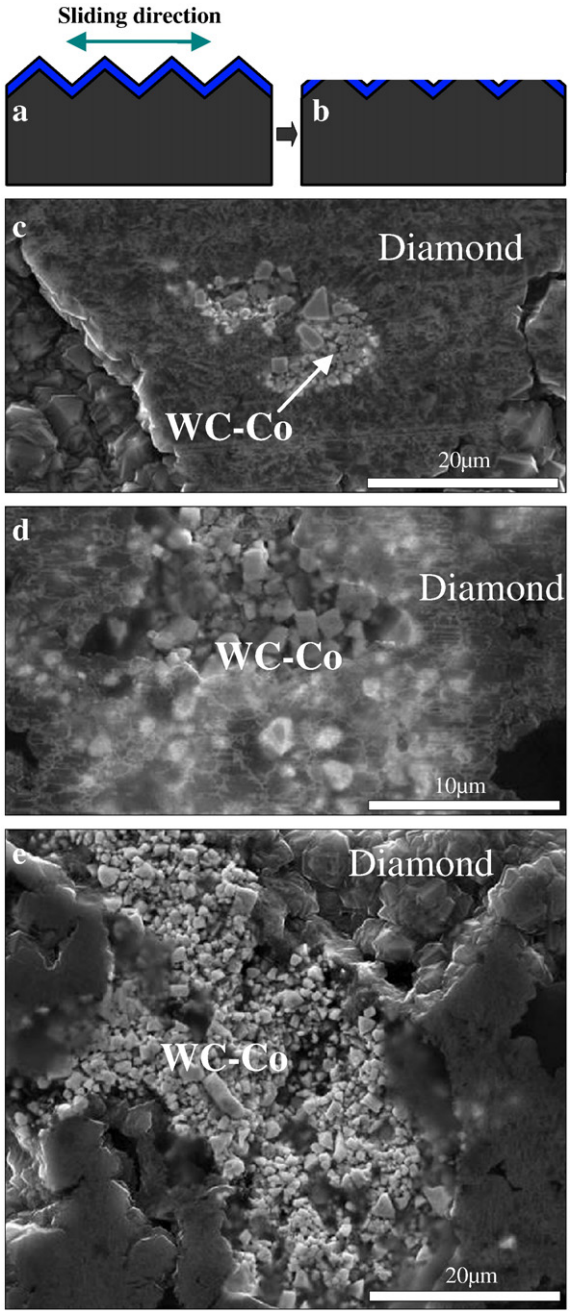

Fig. 7. Fretting wear of thin diamond films deposited on a WC-Co interlayer (*i.e.* specimens D_1 and D_2). (a) and (b) illustrate the morphology of thin diamond films on a rough substrate surface, before and after fretting wear. (c) and (d) show top view SEM images of thin diamond films worn by slide testing, while (e) shows an area of rough WC-Co interlayer exposed by shearing-off a part of diamond film during slide testing.

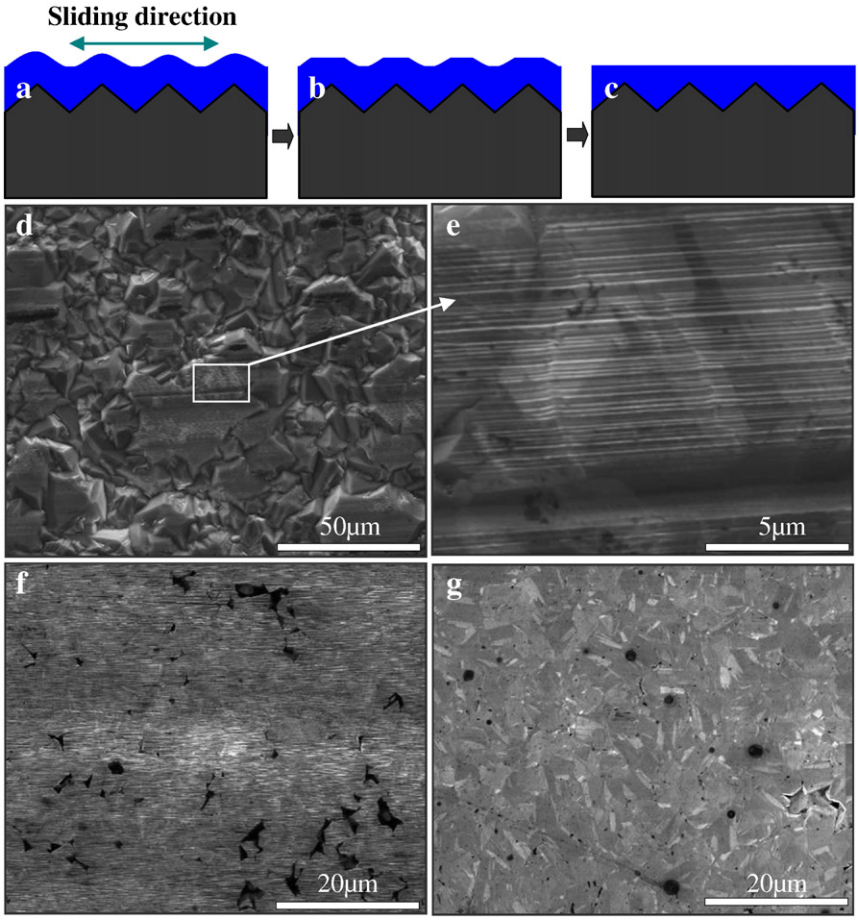

Fig. 8. Fretting wear of thick diamond coatings deposited on a WC-Co interlayer (*i.e.* specimens D_3 and D_4). (a) – (c) illustrate the morphology of a thick diamond film on a rough substrate surface, and its progressive fretting wear. (d) – (g) show top view SEM images of diamond coatings worn and polished by slide testing on D_4 ((d) and (e)) and D_3 ((f) and (g)) Specimens.

polishing) – Fig. 8(b) – followed by more uniform polishing – Fig. 8(c). The accompanying SEM images serve to illustrate such behaviour in the cases of specimens D_4 (Fig. 8(d) and (e)) and D_3 (Fig. 8(f) and (g)).

The progressive evolution of the surface morphology and composition is also revealed through the measured COF values. Fig. 9 shows the COFs of Si_3N_4 balls sliding in air against diamond films of different thickness. Specimen D_1 (with $F=5$ N, $V=500$ rpm) exhibits a COF versus long time (t) dependence that contains features attributable both to film wear and to film flake-off in the period up to ~21200 s (177000 cycles), after which time much of the thin film has been worn away and the COF increases rapidly to >0.20 as shown in Fig. 9(a). The COF of the WC-Co interlayer itself is >0.30, however, implying that some diamond film is still present. Fig. 9(b) shows early time data for another D_1 sample, measured with a larger load ($F=50$ N, $V=500$ rpm). The COF in this case shows a gradual increase, consistent with progressive flaking-off of the thin diamond film (and concomitant decrease in the diamond/WC-Co area ratio). The COF data shown in Fig. 9(c) and (d), for D_2 specimens, show many parallels with that measured with the D_1 samples. The long time COF plot for specimen D_3 (a prototypical example of a thicker diamond film) shown in Fig. 9(e) is consistent with the two stages of fretting wear illustrated in Fig. 8(b) and (c). The present data suggests that surface asperities are fractured and/or smoothed by repeated sliding passes during the run-in period; the magnitude of the microcutting and ploughing contribution to the measured friction therefore decreases with time. As the sliding test continues, the rough microcrystalline diamond film is further polished, and very low COFs are obtained in sliding-contact experiments (Fig. 9 (e)). The contact area of the Si_3N_4 ball on the diamond film in the early stages of a sliding test is very small (approximating a point-contact), ensuring that the sliding test is actually more like a scratch test but, as testing continues, the contact area on the diamond film (both the width and the depth) increases and new asperities on the film surface come into play, and are progressively polished. The normal direction of the sliding trace will experience a longer wear-in period and heavier wear than that of the peripheral zone of the sliding trace. The thickest films (specimen D_4) exhibit larger diamond crystallite sizes (recall Fig. 2) and the COF measurements shown in Fig. 9(f) suggest that, in this case, even after 290000 cycles, the film is still in the polishing stage (Fig. 8(b)), and has not reached the smooth wear stage illustrated in Fig. 8(c).

The SEM, XRD, Raman spectroscopy, Rockwell indentation, electrochemical corrosion and reciprocating fretting wear test results reported in this work serve to emphasize the high quality and good adhesion of diamond films that can be grown on WC-Co coated carbon steel substrates after appropriate chemical pretreatment. WC-Co coatings prove to be a good interlayer for several reasons:

(a) Tungsten forms a carbide, which can be expected to encourage nucleation of diamond seed crystals [45,48];
(b) Thermally sprayed WC-Co coatings provide an excellent combination of wear resistance and high temperature mechanical properties, which are now used extensively in a variety of tribological, corrosion and tribo-corrosion applications [41];
(c) Under the process of diamond growth, diffusion of active atomic carbon encourages transformation of $W_2C \rightarrow WC$ [45], while Co diffusion tends to homogenize the microstructure and phase composition, with the result that the WC-Co interlayer develops a similar microstructure and phase composition to that of bulk sintered WC-Co, and the mechanical properties and corrosion

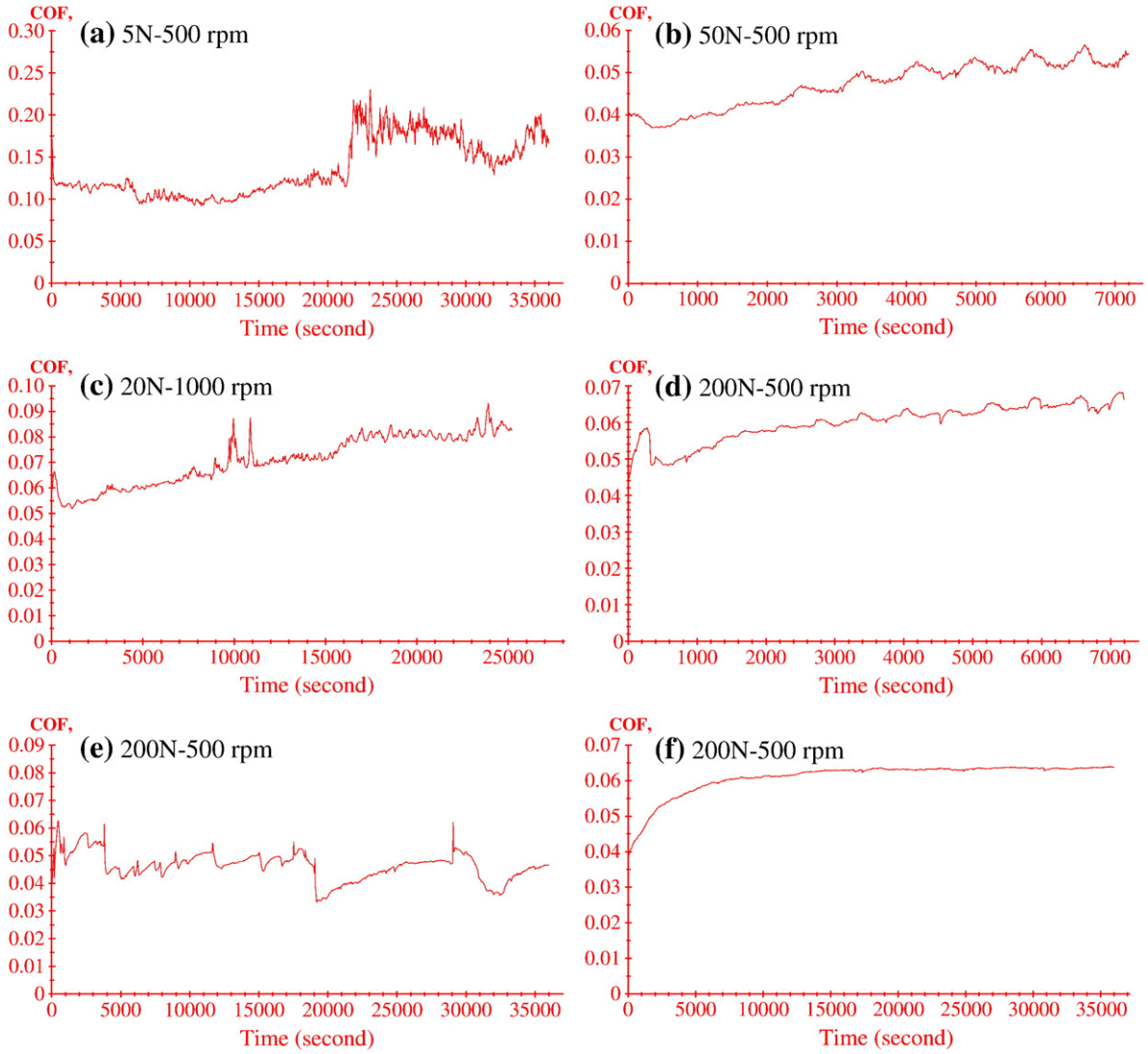

Fig. 9. Measured time dependences of the friction coefficient of Si_3N_4 balls sliding against diamond films on specimens (a, b) D_1, (c, d) D_2, (e) D_3 and (f) D_4. The measurement involved reciprocating sliding tests, performed in ambient air, with respective loads and velocities of (a) 5 N, 500 rpm; (b) 50 N, 500 rpm; (c) 20 N, 1000 rpm; and (d) – (f) 200 N, 500 rpm, with no added lubricant.

resistance of the interlayer will be enhanced. (As an aside, we note that sintered cemented carbide (WC-Co) substrates are widely used in the material forming industry, and CVD diamond films deposited on WC-Co components and tools are already available in the market);

(d) Tungsten carbide interlayers have a low thermal expansion coefficient (relative to many other interlayers), which should be beneficial in reducing the mismatch between the thermal expansion coefficients of diamond and the substrate;

(e) Sliding contact between ductile materials often induces large plastic strains in the near-surface regions, and accumulated plastic strain at the coating/substrate interface can lead to film breakdown [16]. The interposition of a hard, thick WC-Co coating between the ductile steel substrate and a thin diamond film can be expected to reduce any plastic strain in the near-surface regions induced by sliding contact;

(f) Finally, we note that the cost of obtaining a thick WC-Co interlayer by HVOF is lower than that of many other interlayers deposited by physical vapour deposition (PVD) technology.

As Fig. 10 shows, the time dependence of the COF of a D_3 specimen measured by reciprocating slide testing after electrochemical investigation is very different. The COF of this sample is relatively higher at early time but increases rapidly to >0.30 after ~68000 cycles — indicating that the diamond film flaked off at this time. As the sliding test progresses, the pressure P between the diamond film and the Si_3N_4 ball increases steadily, according to the equation $P = F \cdot S$ (where S represents the contact area), which will tend to

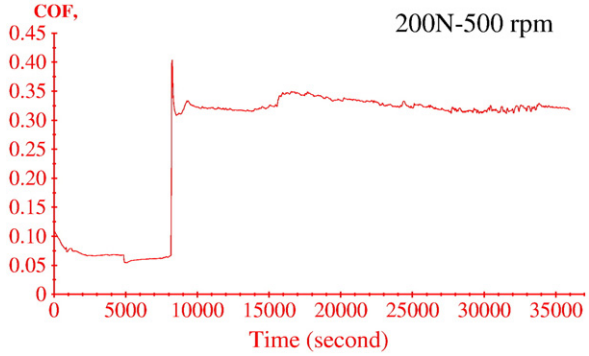

Fig. 10. Evolution of the friction coefficient of a Si_3N_4 ball sliding against a diamond coated D_3 specimen after electrochemical investigation.

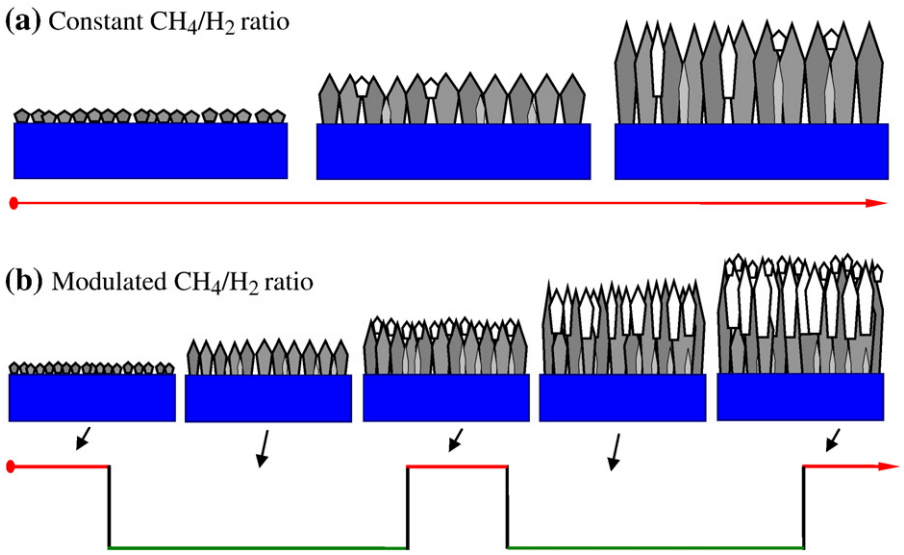

Fig. 11. Pictorial representations of the evolving cross-sectional morphologies of diamond films grown by (a) conventional diamond CVD and (b) time-modulated CVD. The upper horizontal line represents the constant CH_4/H_2 ratio with no change; the lower wavy line represents the CH_4/H_2 ratio in the process gas mixture is cycled in time, the wave crest represents the higher CH_4/H_2 ratio, while the trough represents the lower CH_4/H_2 ratio. The arrows show the developing direction of time.

increase the total shear force on the diamond film. The diamond film will flake-off when the total shear force exceeds the strength of the bonding between the diamond film and the WC-Co interlayer.

The observation of material flake-off also demonstrates that the electrochemical corrosion test degrades the diamond film adhesion. Given the chemical inertness of diamond to acidic, alkaline and saline media, diffusion of water or ions through non-defective diamond crystallites within the coating is very unlikely. However, CVD diamond films generally exhibit a columnar microstructure and a fibrous texture (as illustrated schematically in Fig. 11(a)) [49]. Grain boundaries and packing faults between the columnar structures may provide a route by which the NaCl solution used in the electrochemical studies can penetrate through to the WC-Co/diamond film interface, leading to corrosion of WC-Co at the interface and a decrease in adhesion of the diamond film to the WC-Co interlayer. The present finding that the corrosive potential measured for the diamond coated specimens with a WC-Co interlayer increases with diamond film thickness supports this conjecture. Reuben *et al.* have used X-ray photoelectron spectroscopy methods to investigate electrochemical attack at the silicon/diamond interface, [50] and similar ideas have been advanced in ref. [36]. Buijnsters *et al.* prepared CVD diamond films on tool steel specimens prepared with three different interlayer materials, namely CrN, Si and borided steel, and observed that the corrosion potential was dependent on the choice of interlayer employed [37]. Growth on the CrN coated and borided tool steel specimens resulted in continuous diamond films, but the specimen involving the silicon interlayer exhibited the largest positive corrosion potential; post-deposition analysis showed the CVD coating to comprise a composite layer of carbides and diamond. All of these data support the view that interfacial corrosion can occur by transport through grain boundaries, cracks and microdefects in the diamond coating that are not recognizable by SEM.

Microcrystalline diamond films deposited using conventional CVD methods are rough and exhibit columnar growth characteristics. For smooth substrates, such as single crystalline silicon plate, the average crystallite size and the surface roughness of the as-grown films increase with film thickness – as shown in Fig. 11(a). In an effort to break the continuity of the columnar growth, and achieve a multilayer structure along the lines of that illustrated schematically in Fig. 11(b), the CVD conditions were varied periodically by changing the methane concentration in the process gas mixture (see Table 1). It is well-known that increasing the methane concentration leads to an increase in overall nucleation density, but at the price of degrading film quality (as judged by diamond carbon phase purity). Ali *et al.* [51] reported a time-modulated (TM) CVD process for growing diamond films that offers reduced film roughness, more controlled film microstructure

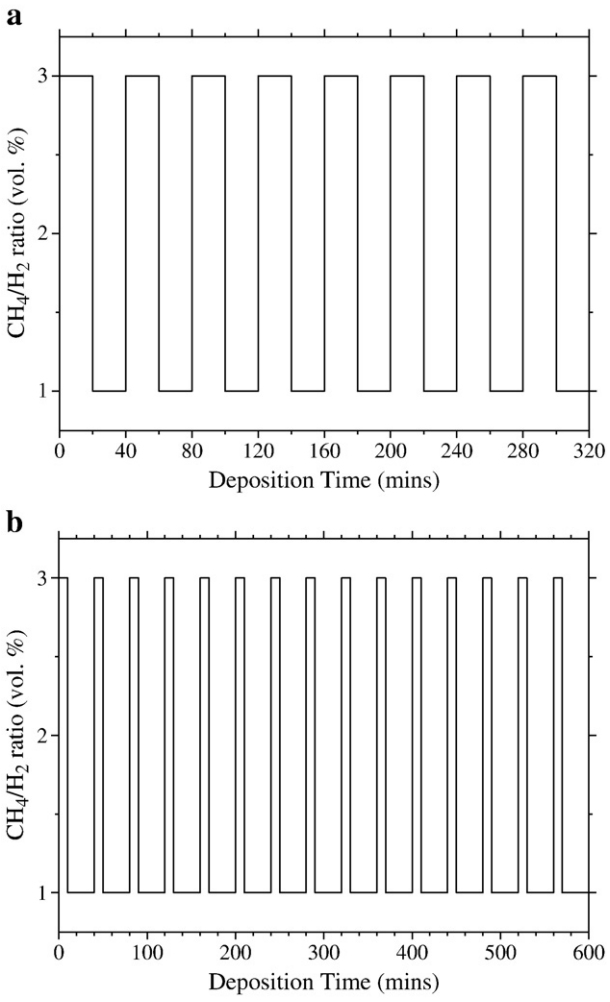

Fig. 12. Variations of the CH_4/H_2 ratio used during TMCVD on specimens (a) D_5 and (b) D_6.

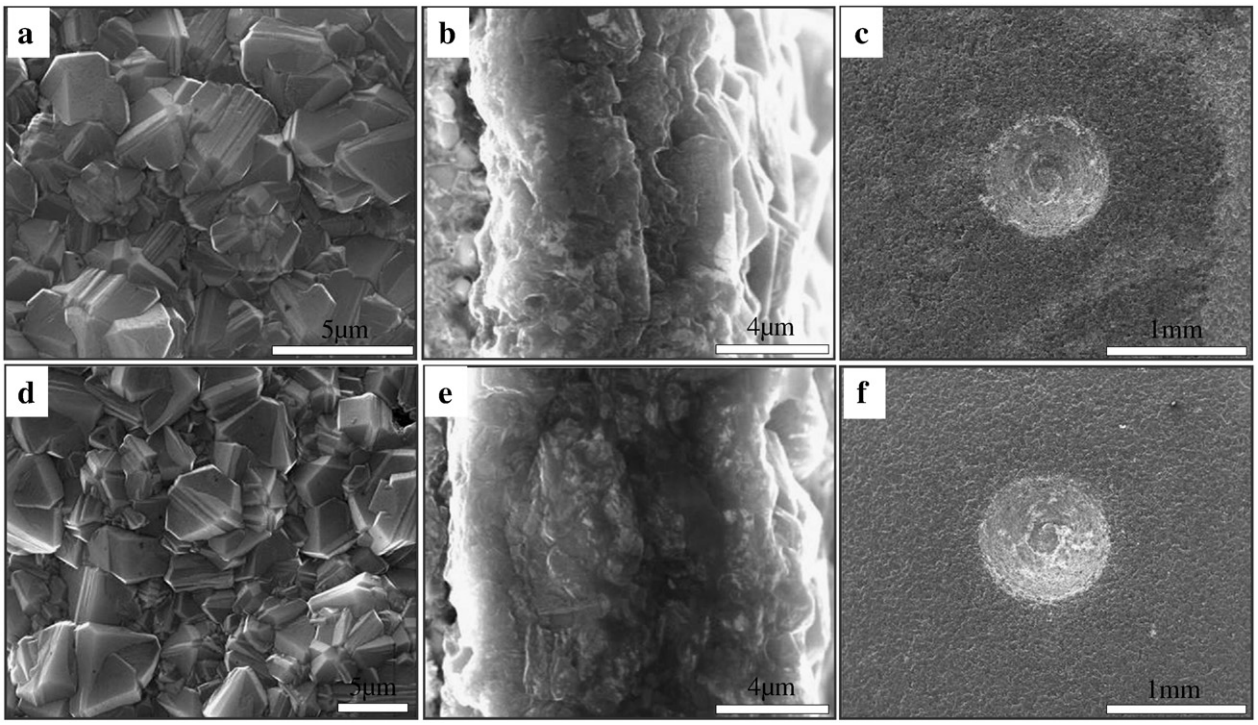

Fig. 13. Representative SEM images of diamond films deposited on specimens D_5 ((a) – (c)) and D_6 ((d) – (f)). Left images are top views, middle images are cross-sections, while right images show the results of Rockwell indentation under a load of 1500 N.

and morphology, and improved film reliability. This procedure has since been applied in a series of related studies [52–57]. The distinctive feature of TMCVD involves switching the CH_4 flow rates and time durations of the CVD process. Fig. 12 shows the variations in CH_4/H_2 ratio (vol. %) during TMCVD of diamond on specimens D_5 and D_6 (*cf* the 3% CH_4/H_2 ratio used during conventional CVD for specimens D_1, D_2, D_3 and D_4). For specimens D_5 and D_6, methane is first introduced into the CVD reactor at a relatively high (3%) CH_4/H_2 ratio for a period of time, then lowered to 1% for another period, then raised again to 3%, and the cycle repeated several times thereafter – hence the term "time-modulated" CVD. Fig. 13 shows representative surface, cross-section and Rockwell indentation SEM images of diamond films grown by TMCVD on specimens D_5 and D_6. The surface SEM images show dense and homogeneous diamond coatings with typical microcrystalline morphologies. Rockwell indentation tests

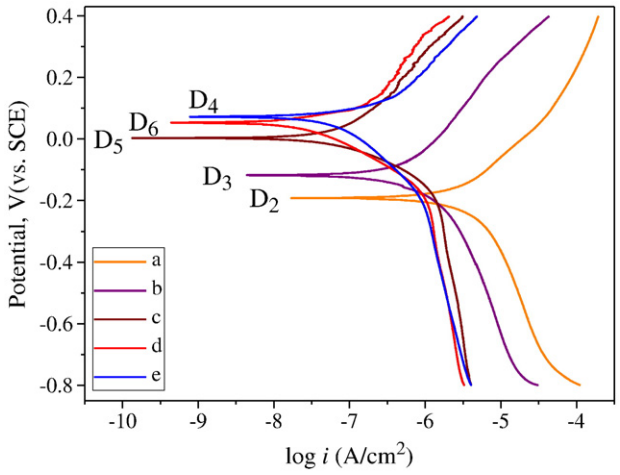

Fig. 14. Comparison of potentiodynamic polarization curves of diamond films deposited on specimens (a) D_2, (b) D_3, (c) D_4, (d) D_5 and (e) D_6 in the aerated 3.5 mol/L NaCl solution.

demonstrate the high quality and good adhesion of both specimens. Fig. 14 shows the electrochemical behaviour of specimens D_5 and D_6. Compared to the specimens D_2 and D_3 (which involve diamond coatings of similar thickness but were deposited under constant process conditions), E_{corr} is shifted significantly in the positive direction; specimen D_6 shows the larger shift, the magnitude of which is comparable to that measured for specimen D_4 – in which the diamond coating thickness is >50 μm. These observations support the view that by periodically varying the process parameters we have succeeded in disrupting the columnar growth and reduced the prevalence of microdefects that act as channels through which corrosive species can penetrate the microcrystalline diamond coatings. Since the initial CH_4/H_2 ratio is the same, and high (3%), the initial nucleation in both environments is similar. In the second stage of the TMCVD process, however, when the CH_4/H_2 ratio is reduced, the diamond crystals grow with better quality. The third stage involves restoration of the higher (3%) CH_4/H_2 ratio, as shown in Fig. 12. Varying the CH_4/H_2 ratio in this way is considered to destabilize the growth conditions, *e.g.* the distributions of active gas phase species, the carburization of the HF, the HF and substrate temperatures, and so on, enabling more secondary nucleation between the pre-existing diamond crystals. Further evidence in support of this assertion is provided by the time dependent COFs shown in Fig. 15 for a D_6 specimen after electrochemical investigation measured by reciprocating sliding tests during the stabilization period. Even after 290000 cycles, the COF remains <0.07 – appropriate for a thick, well-adhered diamond sample (*cf* Fig. 9(f)).

4. Conclusions

A WC-Co coating prepared by high velocity oxy-fuel spraying has been used as an intermediate layer on carbon steel substrates to improve the quality and the nucleation density of diamond film grown on these substrates, and to enhance the diamond film adhesion. Reactive diffusion of atomic carbon during diamond CVD at high substrate temperatures ($T_s = 750 \pm 50$ °C) in a CH_4/H_2

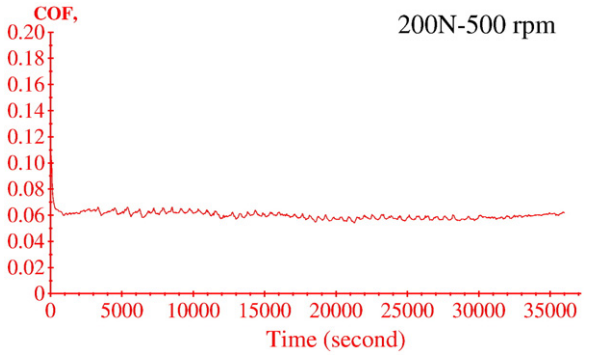

Fig. 15. Evolution of the COF of a Si_3N_4 ball sliding against a diamond film on a D_6 specimen after electrochemical investigation.

atmosphere encourages the transformation $W_2C \rightarrow WC$, while Co binder diffuses from the interlayer to the substrate with the result that the WC-Co interlayer develops a microstructure and phase composition similar to that of bulk sintered WC-Co. WC-Co coatings (after an appropriate chemical pretreatment) are shown to be particularly good interlayers – which are efficient, cost-effective and simultaneously guarantee good adhesion at both the substrate/interlayer and interlayer/diamond interfaces. The dominant wear mechanism for diamond films is shown to depend on the diamond film thickness: thin diamond films will wear out or break-off during high speed, long time reciprocating sliding tests, whereas thicker diamond coatings are initially polished and then wear smoothly. Our preliminary studies suggest that diamond coatings deposited under constant process conditions enhance the electrochemical corrosion resistance of a steel substrate (immersed in 3.5 mol/L NaCl solution), but that electrochemical testing of such specimens reduces adhesion at the diamond/WC-Co interface. This limitation can be circumvented, however, by varying the diamond CVD conditions (*e.g.* the CH_4 flow rate) periodically – which serves to disrupt the columnar structure of the diamond coating and reduce the probability of channeling corrosive solution to the interface. Such diamond coatings grown by time modulated CVD have much to offer for future tribological applications in erosive environments. Relative to most engineering materials, this multilayer material offers a particularly attractive combination of low friction, high hardness, high wear and promising corrosion resistance.

Acknowledgements

The authors wish to thank the “China Scholarship Council”, the “State Key Laboratory of Powder Metallurgy”, the “Outstanding PhD Students Enabling Fund”, the “Innovation Foundation for Postgraduates of Hunan Province of China”, and the “Open Fund for Valuable Instruments of Central South University” for financial support.

References

[1] R.J.K. Wood, Int. J. Refract. Met. H. 28 (2010) 82.
[2] P.K. Bachmann, U. Linz, Adv. Mater. 2 (1990) 195.
[3] M.N.R. Ashfold, P.W. May, C.A. Rego, N.M. Everitt, Chem. Soc. Rev. 23 (1994) 21.
[4] Q.P. Wei, Z.M. Yu, M.N.R. Ashfold, J. Ye, L. Ma, Appl. Surf. Sci. 256 (2010) 4357.
[5] A. Bohner, R. Janisch, A. Hartmaier, Scr. Mater. 60 (2009) 504.
[6] Y.S. Li, A. Hirose, Chem. Phys. Lett. 433 (2006) 150.
[7] E. Nakamura, K.K. Hirakuri, M. Ohyama, G. Friedbacher, N. Mutsukura, J. Appl. Phys. 92 (2002) 3393.
[8] R. Polini, G. Mattei, R. Valle, F. Casadei, Thin Solid Films 515 (2006) 1011.
[9] V.F. Neto, T. Shokuhfar, M.S.A. Oliveira, J. Grácio, N. Ali, Int. J. Nanomanuf. 2 (2008) 99.
[10] J.G. Buijnstersa, P. Shankara, P. Gopalakrishnanb, W.J.P. Van Enckevortc, J.J. Schermerd, S.S. Ramakrishnanb, J.J. Ter Meulena, Thin Solid Films 426 (2003) 85.
[11] A. Fayer, O. Glozman, A. Hoffman, Appl. Phys. Lett. 67 (1995) 2299.
[12] O. Glozman, A. Hoffman, Diam. Relat. Mater. 6 (1997) 796.
[13] J.G. Buijnsters, P. Shankar, W. Fleischer, W.J.P. van Enckevort, J.J. Schermer, J.J. ter Meulena, Diam. Relat. Mater. 11 (2002) 536.
[14] S. Schwarz, S.M. Rosiwal, Y. Musayev, R.F. Singer, Diam. Relat. Mater. 12 (2003) 701.
[15] J.G. Buijnsters, P. Shankar, W.J.P. van Enckevort, J.J. Schermer, J.J. ter Meulen, Diam. Relat. Mater. 13 (2004) 848.
[16] K. Kellermann, C. Bareiß, S.M. Rosiwal, R.F. Singer, Adv. Eng. Mater. 10 (2008) 657.
[17] O. Glozman, A. Berner, D. Shechtman, A. Hoffman, Diam. Relat. Mater. 7 (1998) 597.
[18] C. Bareih, M. Perle, S.M. Rosiwal, R.F. Singer, Diam. Relat. Mater. 15 (2006) 754.
[19] H. Li, M. Gowri, J.J. Schenner, W.J.P. van Enckevort, T. Kacsich, J.J. ter Meulen, Diam. Relat. Mater. 16 (2007) 1918.
[20] V.F. Neto, R. Vaz, N. Ali, M.S.A. Oliveira, J. Gracio, Diam. Relat. Mater. 17 (2008) 1424.
[21] R. Haubner, B. Lux, Int. J. Refract. Met. H. 24 (2006) 380.
[22] B. Bhushan, V.V. Subramaniam, A. Malshe, B.K. Gupta, J. Ruan, J. Appl. Phys. 74 (1993) 4174.
[23] A. Erdemir, C. Bindal, G.R. Fenske, C. Zuiker, A.R. Krauss, D.M. Gruen, Diam. Relat. Mater. 5 (1996) 923.
[24] A. Erdemir, M. Halter, G.R. Fenske, A.R. Krauss, D.M. Gruen, S.M. Pimenov, V.I. Konov, Surf. Coat. Technol. 91–95 (1997) 537.
[25] A. Erdemir, G.R. Fenske, A.R. Krauss, D.M. Gruen, T. McCauley, R.T. Csencsits, Surf. Coat. Technol. 120–121 (1999) 565.
[26] Y. Fu, B. Yan, N.L. Loh, C.Q. Sun, P. Hing, Mater. Sci. Eng. A282 (2000) 38.
[27] F.J.G. Silva, A.J.S. Fernandes, F.M. Costa, V. Teixeira, A.P.M. Baptista, E. Pereira, Wear 255 (2003) 846.
[28] C.S. Abreu, F.J. Oliveira, M. Belmonte, A.J.S. Fernandes, R.F. Silvab, J.R. Gomes, Wear 259 (2005) 771.
[29] C.S. Abreu, F.J. Oliveira, M. Belmonte, A.J.S. Fernandes, J.R. Gomes, R.F. Silva, Tribol. Lett. 21 (2006) 141.
[30] A. Schade, S.M. Rosiwal, R.F. Singer, Surf. Coat. Technol. 201 (2007) 6197.
[31] F. Mubarok, J.M. Carrapichano, F.A. Almeida, A.J.S. Fernandes, R.F. Silva, Diam. Relat. Mater. 17 (2008) 1132.
[32] C.S. Abreu, E. Salgueiredo, F.J. Oliveira, A.J.S. Fernandes, R.F. Silvab, J.R. Gomes, Wear 265 (2008) 1023.
[33] M. Amaral, C.S. Abreu, F.J. Oliveira, J.R. Gomes, R.F. Silva, Diam. Relat. Mater. 17 (2008) 848.
[34] C.C. Chou, J.W. Lee, Y.I. Chen, Surf. Coat. Technol. 203 (2008) 704.
[35] A. Schneider, D. Steinmueller-Nethl, M. Roy, F. Franek, Int. J. Refract. Met. H. 28 (2010) 40.
[36] I. Garcia, A. Conde, J.J. De Damborenea, A.J. Vazquez, Thin Solid Films 310 (1997) 217.
[37] J.G. Buijnsters, R.V. Subba Rao, P. Shankar, W.J.P. van Enckevort, J.J. Schermer, A. Gebert, J.J. ter Meulen, Surf. Coat. Technol. 191 (2005) 119.
[38] M. Gowri, W.J.P. van Enckevort, J.J. Schermer, J.P. Celis, J.J. ter Meulen, J.G. Buijnsters, Diam. Relat. Mater. 18 (2009) 1450.
[39] Z. Yu, U. Karlsson, A. Flodstrom, Thin Solid Films 342 (1999) 74.
[40] M.G. Peters, R.H. Cummings, in: E. Patent (Ed.) European Patent vol. 0519587 1992, p. A1.
[41] D.A. Stewart, P.H. Shipway, D.G. McCartney, Adv. Mater. 48 (2000) 1593.
[42] M.R. Thakare, J.A. Wharton, R.J.K. Wood, C. Menger, Tribol. Int. 41 (2008) 629.
[43] S.F. Wayne, S. Sampath, J. Thermal Spray Technol. 1 (1992) 307.
[44] M.M. Lima, C. Godoy, J.C. Avelar-Batista, P.J. Modenesi, Mater. Sci. Eng. A357 (2003) 337.
[45] Q.P. Wei, Z.M. Yu, L. Ma, D.F. Yin, J. Ye, Appl. Surf. Sci. 256 (2009) 1322.
[46] J.B. Donnet, D. Paulmier, H. Oulanti, T. Le Huu, Carbon 42 (2004) 2215.
[47] R. Polini, P. D'Antonio, S. Lo Casto, V.F. Ruisi, E. Traversa, Surf. Coat. Technol. 123 (2000) 78.
[48] V.G. Ralchenko, A.A. Smolin, V.G. Pereverzev, E.D. Obraztsova, K.G. Korotoushenko, V.I. Konov, Y.V. Lakhotkin, E.N. Loubnin, Diam. Relat. Mater. 4 (1995) 754.
[49] P. Smereka, X. Li, G. Russo, D.J. Srolovitz, Adv. Mater. 53 (2005) 1191.
[50] C. Reuben, E. Galun, H. Cohen, R. Tenne, R. Kalish, Y. Muraki, K. Hashimoto, A. Fujishima, M.J. Butler, J. Electroanal. Chem. 396 (1995) 233.
[51] N. Ali, Q.H. Fan, W. Ahmed, J. Grácio, Thin Solid Films 420–421 (2002) 155.
[52] N. Ali, Q.H. Fan, Y. Kousar, W. Ahmed, J. Grácio, Vacuum 71 (2003) 445.
[53] N. Ali, V.F. Neto, J. Grácio, J. Mater. Res. 18 (2003) 296.
[54] N. Ali, V.F. Neto, S. Mei, G. Cabral, Y. Kousar, E. Titus, A.A. Ogwu, D.S. Misra, J. Grácio, Thin Solid Films 469–470 (2004) 154.
[55] N. Ali, G. Cabral, A.B. Lopes, J. Grácio, Diam. Relat. Mater. 13 (2004) 495.
[56] M.J. Jackson, G.M. Robinson, W. Ahmed, H. Sein, A.N. Jones, N. Ali, E. Titus, Q.H. Fan, J. Grácio, J. Mater. Sci. Eng. Perform. 14 (2005) 163.
[57] V.F. Neto, M.S.A. Oliveira, N. Ali, J. Grácio, Vacuum 82 (2008) 1346.